

# Localization of Receivers using Phased-Array Wireless Power Transfer Systems

Vaishnavi Ranganathan<sup>1</sup>, Benjamin H. Waters<sup>1</sup>, Joshua R. Smith<sup>2,1</sup>

[1]Electrical Engineering Department [2]Computer Science and Engineering Department  
University of Washington; Seattle, WA 98195

## Abstract—

Wireless battery charging has been incorporated into an increasing number of commercial electronics with power requirements ranging from a few milliwatts to several hundred watts. With this growing number of deployed devices, there is a necessity to quickly locate and charge them individually. Conventional localization techniques either require intelligence and extra hardware or are limited to merely detecting the presence of an object and not its position. In the proposed localization technique, we use two wireless power transmitters (TX) operating at the same frequency. The phase difference between the two TXs can be controlled. The forward/reflected signals are measured from each TX and this information is used to accurately localize the receiver in a two dimensional space. This system does not require additional hardware on the TX or RX side. The entire detection process can be confined to the transmitter firmware. We also formulate a simple localization parameter using the reflected signals to prove the concept of localization.

**Index Terms**—Wireless power transfer (WPT), resonators, near field, localization, reflected power.

Localization of objects in space has been a topic of interest in various application like medicine, geology and electronics. To address these applications techniques such as radar, ultrasound, radio frequency [1] and other electrical systems have been predominantly used. Most of these consist of one or more transmitters (TX) and receivers (RX) which communicate with each other to localize. In near field WPT, localization is of increased significance as the power levels can be very high and hence it is ideal to transmit power only to the targeted receive device. The reasons are primarily to conserve power and to not transmit when human beings and other objects are in close proximity.

WPT systems mostly consist of one TX and one RX coil. Recent work has demonstrated WPT with multiple TX-RX coils [2]. With a single TX system, localization is done by having the RX inform the TX of its position, or use other position sensing hardware. This is primarily due to insufficient information gained from the reflected signal with a single TX. In this work we leverage the phase difference between the two TXs to achieve localization. Keeping the magnitude of the power on both TXs constant, phase on TX<sub>2</sub> is swept relative TX<sub>1</sub> and the magnitude and phase of the forward/reflected power are recorded. This method uses a directional coupler and digital signal processor (DSP) present on a TX power amplifier (PA) for the entire task. This also eliminates the necessity for incorporating additional hardware dedicated to localization.

## I. THEORY

Using an array of TXs to implement WPT systems has recently been adopted for achieving better efficiency and range in near field WPT [3] [4]. In such multi-TX cases, the magnitude and phase of TXs are swept to obtain constructive and destructive interference for location-selectable power delivery. The circuit level analysis of multi-transmitter topologies are discussed in detail in [5]. A similar method is presented in this work which uses two TX coils and one RX coil to achieve localization of the RX in a 2D space. The goal for this work is to localize an RX by using the existing hardware on the TX side and eliminating the dependence on RX communication.

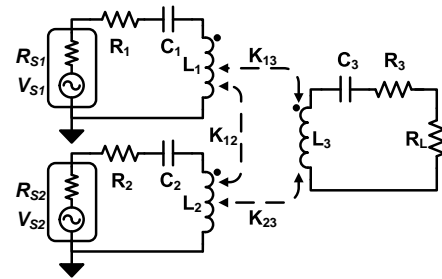


Fig. 1. Circuit representation of a three coil system.

### A. Circuit configuration

The equivalent circuit schematic for a three coil system with two TX coils and one RX coil is shown in Fig.1. [6] describes the circuit and forward/reflected characteristics for a multi coil system. Both the TX PAs are configured to deliver the same magnitude of power into a  $50\Omega$  load.  $V_{S1} = \cos(\omega t)$  and  $V_{S2} = \alpha \cos(\omega t + \phi)$ , where  $\alpha$  and  $\phi$  represent the magnitude and phase on TX<sub>2</sub>. The resonant frequency for power transfer was chosen to be 13.56MHz. The TX coils and the RX coil are all identical with inductance  $L = 17.2\mu H$ , series capacitance  $C = 8pF$  and AC resistance  $R = 1.2\Omega$ .

### B. Experimental setup

In the following experiments both TXs are powered by individual custom made class-E PA PCBs. The schematic design and the setup are shown in Fig.2A and B. The RX is connected to a power meter through a  $50\Omega$  attenuator. A directional coupler at the output of the PA passes the forward and reflected signals to an RF detector. The detector measures

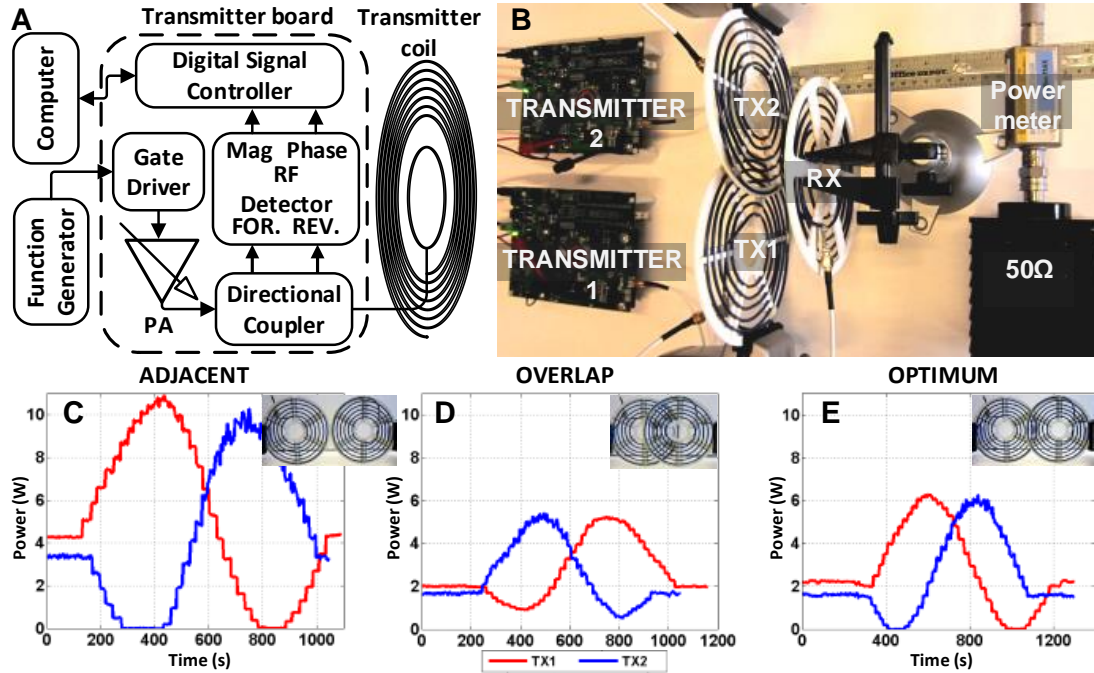


Fig. 2. (A) Schematic of transmitter, (B) Experimental setup, TX power variation over time during phase sweep for (C) Adjacent, (D) Overlap, and (E) Optimal configurations.

the magnitude and phase difference between the forward and reflected signals. We refer to this as the S11 parameter that is used to localize the RX position. The PAs are controlled by output ports on a Tektronix AFG3252 dual channel function generator. The TX boards initially carry out a standard  $\phi$  sweep from  $-180^\circ$  to  $180^\circ$  while RX is absent. The RX can be localized by analyzing the S11 parameters at each  $\phi$  sweep. The PA control interface logs the S11 data which is parsed using Matlab and compared for localization, however, this calculation could be done in real time on the DSP. For 2D localization, the space in front of the TX coils is divided into multiple positions which will be explained in the following sections. The RX coil is placed parallel to the TX coils.

## II. EXPERIMENTAL ANALYSIS

A favorable TX configuration is identified and used for the localization experiments. The following experiments are carried out with two TX coils to maintain simplicity.

### A. Optimal TX configuration

Before proceeding with the experiments, it is important to identify an optimal configuration for the two TX coils. High TX coupling ( $k_{12}$ ) results in high power dissipation even when RX is absent but has good S11 correlation for localization. Whereas, very low  $k_{12}$  implies low power dissipation but also less correlation between the S11 and different locations of RX. Two different TX coil arrangements were initially considered. In the first arrangement the TX coils are placed adjacent to each other (ADJ), and in the second they overlap (OVL) by more than 50 % as shown in the insets of Fig.2C and D.

The drive strength of both TXs was 5Vpp. Phase of TX<sub>1</sub> was set to 0 and  $\phi$  was swept. From the standard TX power levels plotted in Fig.2, it is evident that ADJ consumes higher power (11W) when compared to OVL (5.5W). This is primarily because, in the ADJ configuration, the transmitters are strongly coupled. While in OVL  $k_{12}$  is very poor and hence there is less power transferred across the TX coils. Also, due to the excellent  $k_{12}$  localization is easier in the ADJ configuration. To identify a configuration with low power dissipation as well as good localization ability a set of standard measurements were obtained for several configurations and the optimal case was selected as shown in Fig.2E.

### B. Localization experiment

To identify a method of localizing the RX, a second set of experiments are performed. The PAs are both driven by the function generator. The phase of TX<sub>1</sub> is set at  $-180^\circ$  and  $\phi$  is swept from  $-180^\circ$  to  $180^\circ$  at  $2^\circ$  increments using a python controller interface to the AFG3252. S11 magnitude and phase are recorded at each  $\phi$  setting. For 2D localization in this experiment, the space in front of the TX coils is divided into 3 positions at three distances; in front of TX<sub>1</sub> (POS1), between the TX coils (POS2), and in front of TX<sub>2</sub> (POS3). Each position at distances of 3cm, 6cm and 9cm from the TX coils represents overcoupled, critically coupled and undercoupled regions respectively, as shown in the picture above Fig.3. The RX coil is placed parallel to the TX coils at each of the nine positions depicted by circles in the picture.

Fig.3 shows the recorded S11 magnitude plotted on the y axis with the phase sweep in radians on the x axis. Similarly

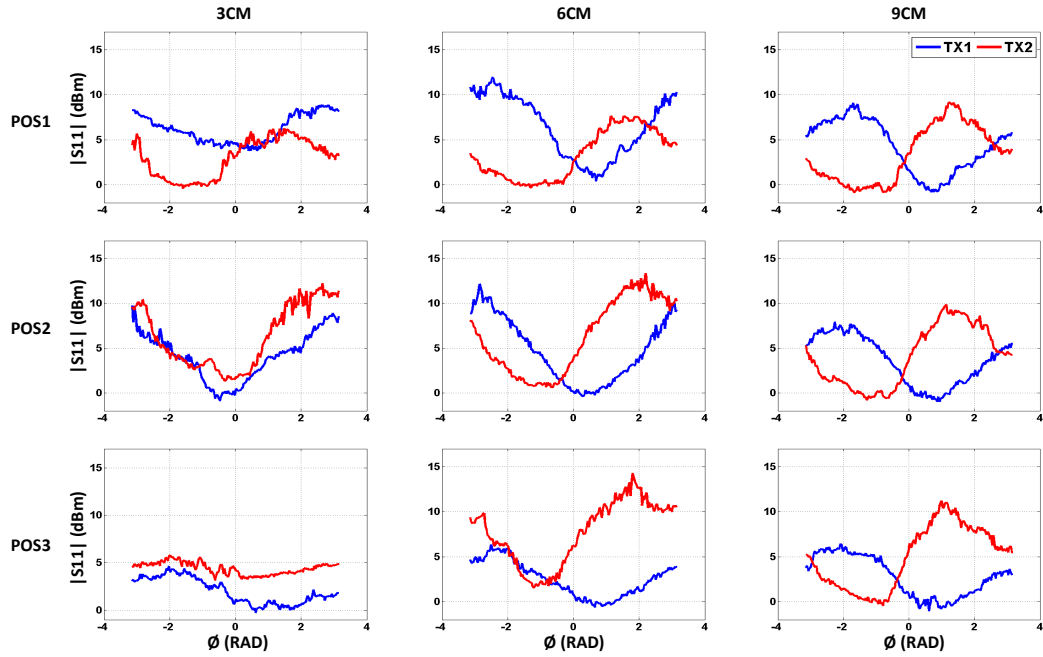
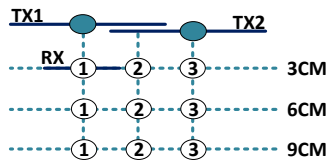


Fig. 3. S11 Magnitude plots over phase for nine RX positions.

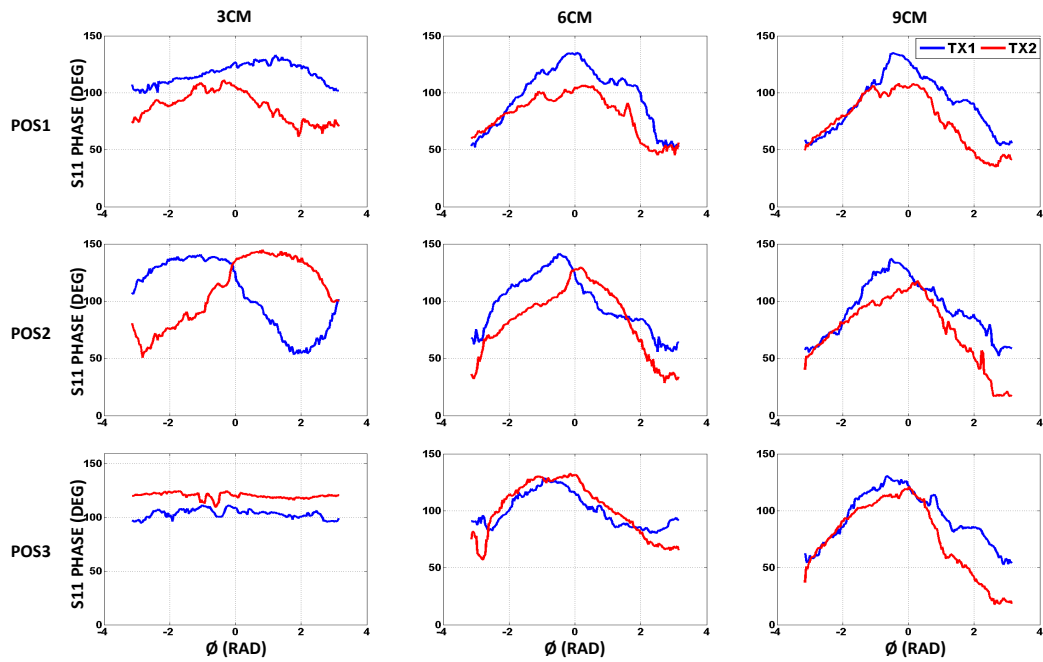


Fig. 4. S11 phase plots over phase for nine RX positions.

Fig.4 presents the S11 phase data on the y-axis with phase sweep on the x-axis. This data represents the S11 values averaged over two trials. In the 3cm distance, when the RX is placed in front of TX<sub>1</sub>, both S11 phase and magnitude of TX<sub>1</sub> are greater than that of TX<sub>2</sub> (POS1), similarly when RX is placed in front of TX<sub>2</sub> (POS3). However, if RX is centrally located between the two TX coils, there is no clear distinction between their S11 magnitudes and the shift in phase signals reflect the position to some extent(POS2). A similar trend can be observed in the 6cm plots. It is clear that both phase and magnitude are necessary to identify the positions at the different distances. This point becomes clear in the 9cm configurations as it can be distinguished from the other two distances based on magnitude, but differentiating between the three positions by simple comparisons is challenging. This is because the RX is now in the undercoupled region where the S11 signals are small and very close to the standard without any RX.

To make localization achievable within the given range, a localization parameter (*LOC*) was formulated to localize the RX based the S11 data of each TX. A shape dependent centroid was first calculated for the magnitude and phase curves of S11 based on (1). Where, R represents the centroid, A is the amplitude of the curve at point B across the phase sweep, for each of the traces. R is computed over the *i* samples in the trace. For all nine configurations the *LOC* point was computed as given in (3). Where,  $R_{M1}$ ,  $R_{M2}$ ,  $R_{PH1}$  and  $R_{PH2}$  stand for the centroid of magnitude and phase of the two TXs respectively.

$$R = \frac{1}{\sum_{i=1}^n A_i} \left\{ \sum_{i=1}^n (A_i)(B_i) \right\} \quad (1)$$

$$X = R_{PH2} - R_{PH1}, \quad Y = R_{M2} - R_{M1} \quad (2)$$

$$LOC = (X, Y) \quad (3)$$

The *LOC*s of all nine configurations are plotted in Fig.5A. The x-axis is the difference in the phase centroid (*X*) and the y-axis is the difference in magnitude centroid of each location (*Y*). The constellation in red, blue and green represents the three distances 3cm, 6cm and 9cm. POS1, POS2 and POS3 are represented by circle, star and square markers respectively. The constellations for the three distances can be clearly distinguished in space and these are used as reference locations. A separate set of experiments were then performed by placing the RX at approximately the same nine positions and S11 data is recorded with  $\phi$  sweeps at 2° increments. This is followed by another set of measurements made with  $\phi$  sweeps at 3° increments. The first set of data has 180 data points, while the second set has only 120. These experiments are used to verify that the RX can be localized consistently with repeatability and also to estimate the effect of varying number of data points. The *LOC* points for the recorded S11 data are computed in the same way as mentioned above. Three positions are chosen for the 2° sweeps; they were approximately POS1 at 3cm, POS2 at 6cm and POS3 at 9cm. The cyan markers

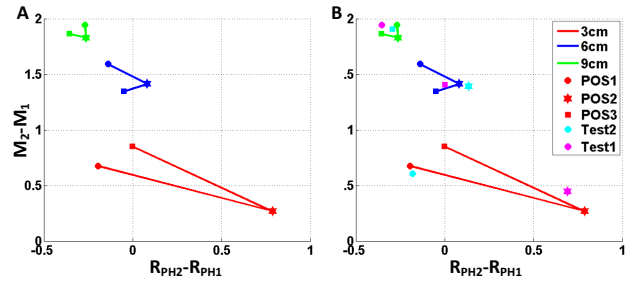


Fig. 5. (A) *LOC* constellation plot showing three different distances (B) Test case localization points for 2° and 3° sweep interval

in Fig.5B represent these results and the estimates closely match the actual position. Similarly, three positions are chosen for the 3° sweeps; they were approximately POS2 at 3cm, POS3 at 6cm and POS1 at 9cm. The purple markers on Fig.5B represent these locations. They also closely match the actual positions. Therefore, we can confirm that variance in the number of points in the  $\phi$  sweep does not impact the localization accuracy. A shortest distance vector can be used to localize the RX precisely around one of the reference locations. This simple algorithm can be run on a DSP to approximately locate the RX without additional out-of-band communication dependence.

### III. CONCLUSION

This work uses a two TX, single RX phased array system, to achieve 2D localization of a receiver in near-field WPT systems. An optimal arrangement of TX coils was considered for this process to enable lower power dissipation and accurate localization. The localization mechanism leverages the difference in phase and magnitude of the forward/reflected power on each TX and also its difference from a standard measurement without any RX. A simple algorithm was developed to be run on the TX side and tested for localization of the RX, thus eliminating the dependence on communication with RX.

### REFERENCES

- [1] L. Ni, D. Zhang, and M. Souryal, "Rfid-based localization and tracking technologies," *Wireless Communications, IEEE*, vol. 18, no. 2, pp. 45–51, April 2011.
- [2] R. Johari, J. Krogmeier, and D. Love, "Analysis and practical considerations in implementing multiple transmitters for wireless power transfer via coupled magnetic resonance," *Industrial Electronics, IEEE Transactions on*, vol. 61, no. 4, pp. 1774–1783, April 2014.
- [3] N. Oodachi, K. Ogawa, H. Kudo, H. Shoki, S. Obayashi, and T. Morooka, "Efficiency improvement of wireless power transfer via magnetic resonance using transmission coil array," in *Antennas and Propagation (APSURSI), 2011 IEEE International Symposium on*, July 2011, pp. 1707–1710.
- [4] B. Waters, B. Mahoney, V. Ranganathan, and J. Smith, "Power delivery and leakage field control using an adaptive phased-array wireless power system," *Power Electronics, IEEE Transactions on*, vol. PP, no. 99, pp. 1–1, 2015.
- [5] D. Ahn and S. Hong, "Effect of coupling between multiple transmitters or multiple receivers on wireless power transfer," *Industrial Electronics, IEEE Transactions on*, vol. 60, no. 7, pp. 2602–2613, July 2013.
- [6] B. H. Waters, A. P. Sample, and J. R. Smith, "Adaptive impedance matching for magnetically coupled resonators," *PIERS Proceedings*, pp. 694–701, August 2012.